

Principles of Data Science Project 4

Domain Adaptation

Hongzhou Liu
517030910214

deanlh@sjtu.edu.cn

Xuanrui Hong
517030910227

hongxuanrui.1999@sjtu.edu.cn

Qilin Chen
517030910155

1017856853@sjtu.edu.cn

Abstract—In this project, we tried different domain adaptation methods on the Office-Home dataset, which contains 65 categories of things from 4 domains. The four domains are Art, Clipart, Product and Real-World. In our experiments, we take Art, Clipart and Product as source domains and Real-World as target domain. For traditional methods, we tried KMM, CORAL, GFK, TCA, and EasyTL. For deep learning methods, we only tried DAN due to the scarce of computation resources and time limitation. We compared performances among those methods and discussed the difference among them.

Index Terms—Domain Adaptation, Transfer Learning

I. INTRODUCTION

In this project, we tried different unsupervised domain adaptation methods on the Office-Home dataset, which contains 65 categories of things from 4 domains. The four domains are Art, Clipart, Product and Real-World. There are two parts in this section. Firstly, we will introduce several traditional transfer learning methods we used in our project, including KMM, CORAL, GFK TCA and EasyTL. Then we will introduce deep transfer learning method DAN to compare with the traditional transfer learning methods.

A. Transfer Component Analysis (TCA)

For domain adaptation, Transfer Component Analysis (TCA) [1] tries to learn some transfer components across domains in a Reproducing Kernel Hilbert Space (RKHS) using Maximum Mean Discrepancy (MMD). It minimizes the distance between domain distributions by projecting data onto the learned transfer components.

The basic assumption of TCA is

$$P(X_s) \neq P(X_t)$$

where X_s denotes source domain data and $P(X_s)$ denotes its marginal distributions, X_t denotes target domain data and $P(X_t)$ denotes its marginal distributions. The motivation of TCA is to find a map Φ which could preserve the most data properties after projection, which means obtain the most variance, i.e.

$$P(\phi(\mathbf{x}_s)) \approx P(\phi(\mathbf{x}_t))$$

or we can find conditional distribution of the two will also be similar as:

$$P(y_s | \phi(\mathbf{x}_s)) \approx P(y_t | \phi(\mathbf{x}_t))$$

We can give the maximum mean discrepancy (MMD) formula as:

$$MMD(X, Y) = \left\| \frac{1}{n_1} \sum_{i=1}^{n_1} \Phi(x_i) - \frac{1}{n_2} \sum_{j=1}^{n_2} \Phi(y_j) \right\|^2$$

where n_1, n_2 are the number of instances of the two domains. Then by changing the solution of this function to the solution of the kernel function, we can get:

$$\text{Dist}(X'_S, X'_T) = \text{tr}(KL)$$

where

$$K = \begin{bmatrix} K_{S,S} & K_{S,T} \\ K_{T,S} & K_{T,T} \end{bmatrix} \in \mathbb{R}^{(n_1+n_2) \times (n_1+n_2)}$$

, then, Q Yang [1] decomposed K to transfer this problem to:

$$\begin{cases} \min \text{tr}(W^T K L K W) + \mu \text{tr}(W^T W) \\ \text{s.t. } W^T K H K W = I_m \end{cases}$$

Finally, we can get the solution W^* as the m leading eigenvectors of

$$(K L K + \mu I)^{-1} K H K$$

B. Easy Transfer Learning (EasyTL)

Most traditional and deep learning migration algorithms are parametric methods, which require a lot of time and money to train those hyperparameters. In order to overcome these drawbacks, Easy Transfer Learning (EasyTL) [2] learns non-parametric transfer features through intra-domain alignment, and learns transmission classification through intra-domain programming. EasyTL can also improve the performance of existing TL methods through in-domain programming as the final classifier, the procedure of EasyTL can be shown in Fig. I-B.



Fig. 1. procedure of EasyTL [2]

C. Deep Adaptation Network (DAN)

Recent research shows that deep neural networks can learn transferable features, which can be well extended to new fields to adapt to tasks. Deep Adaptation Network (DAN) use deep net to optimize the loss function and distribution distance in Regenerative Nuclear Hilbert Space (RKHS) [3].

Denote \mathcal{H}_k as the reproducing kernel Hilbert space (RKHS) endowed with a characteristic kernel k . The average embedding of the distribution p in \mathcal{H}_k is a unique element $k(p)$, making $\mathbf{E}_{\mathbf{x} \sim p}(f(\mathbf{x})) = \langle f(\mathbf{x}), \mu_k(p) \rangle_{\mathcal{H}_k}$ for all $f \in \mathcal{H}_k$. Define the MK-MMD $d_k(p, q)$ between the probability distributions p and q as the average embedding distance RKHS of p and q , and define the square formula of MK-MMD as

$$d_k^2(p, q) \triangleq \|\mathbf{E}_p[\phi(\mathbf{x}^s)] - \mathbf{E}_q[\phi(\mathbf{x}^t)]\|_{\mathcal{H}_k}^2$$

and the kernel defined by the multiple cores is

$$\mathcal{K} \triangleq \left\{ k = \sum_{u=1}^m \beta_u k_u : \sum_{u=1}^m \beta_u = 1, \beta_u \geq 0, \forall u \right\}$$

Global optimization goal consists of two parts: loss function and distribution distance. The loss function is used to measure the difference between the predicted value and the true value.

DAN use adaptive method based on mk-mmd and CNNs to overcome that the target domain has no or only limited label information, so it is impossible to adapt CNN directly to the target domain through fine-tuning, or it is easy to overfit. Fig. I-C gives a description of the proposed DAN model.

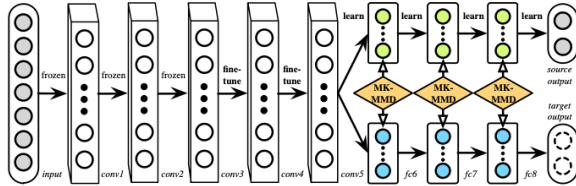


Fig. 2. The DAN architecture for learning transferable features. Since deep features eventually transition from general to specific along the network, (1) the features extracted by convolutional layers conv1conv3 are general, hence these layers are frozen, (2) the features extracted by layers conv4conv5 are slightly less transferable, hence these layers are learned via fine-tuning, and (3) fully connected layers fc6fc8 are tailored to fit specific tasks, hence they are not transferable and should be adapted with MK-MMD. [3]

DAN fine-tuned the source of the labeled examples, requiring that under the hidden representation of the fully connected layers $f_{c6} f_{c8}$, the distribution of the source and target becomes similar. This can be achieved by adding a multi-layer adaptive regularizer (1) based on mk-mmd to the risk (3) of CNN:

$$\min_{\Theta} \frac{1}{n_a} \sum_{i=1}^{n_a} J(\theta(\mathbf{x}_i^a), y_i^a) + \lambda \sum_{\ell=l_1}^{l_2} d_k^2(\mathcal{D}_s^\ell, \mathcal{D}_t^\ell)$$

where $\lambda > 0$ is a penalty parameter, l_1 and l_2 are layer indices between which the regularizer is effective.

D. Traditional Transfer Learning Methods

1) *Kernel Mean Matching (KMM)*: Huang et al. proposed Kernel Mean Matching [4] to estimate the probability density of data samples. The ultimate goal is to weight the samples to make the probability distribution of source domain and target domain closer. The core of the method is the measurement of the difference in the distribution of the two areas. Specifically, the weighted data of the two areas is mapped into the RKHS, and the difference between the average values of the samples in each area is obtained. This distribution measurement method is called the maximum mean difference. After learning the weights of samples with similar distributions, standard machine learning algorithms can be trained and predicted. For example, using SVM:

$$\text{step1: } \min_{\beta_i} \left\| \frac{1}{n_s} \sum_{i=1}^{n_s} \beta_i \phi(x_i^s) - \frac{1}{n_t} \sum_{i=1}^{n_t} \phi(x_i^t) \right\|^2 \quad (1)$$

$$\text{step2: } \min_{w, b, \xi_i} \frac{1}{2} \|w\|^2 + C \sum_i \beta_i \xi_i \quad (2)$$

$$\text{s.t. } y_i(w^T \phi(x_i) + b) \geq 1 - \xi_i, \xi_i \geq 0, \forall i \quad (3)$$

2) *CORrelation ALignment (CORAL)*: The goal of CORAL is to minimize the second-order distance between source domain and target domain, that is, covariance.

The main formula is as follows:

$$\min_A \left\| \widehat{C}_s - C_t \right\|_F^2 = \min_A \left\| A^T C_s A - C_t \right\|_F^2 \quad (4)$$

$$C_s = U_s \Sigma_s U_s^T, C_t = U_t \Sigma_t U_t^T \quad (5)$$

The optimal solution:

$$A^* = U_s \Sigma_s^{-\frac{1}{2}} U_s^T U_t [1:r] \Sigma_t [1:r]^{\frac{1}{2}} U_t [1:r]^T \quad (6)$$

$$r = \min(\text{rank}(C_s), \text{rank}(C_t)) \quad (7)$$

3) *Geodesic Flow Kernel (GFK)*: Geodesic Flow Kernel's [5] main idea based on the Domain Adaption method of geodesic flow cores (preferably displayed in color). They embed the source data set and the target data set into the Glassman manifold. Then, they construct a flow between two points of the geodesic line and integrate the infinite flow (t) in the subspace. Specifically, the original features are projected into these subspaces to form an infinite dimensional feature vector z_h . The inner product between these feature vectors defines a kernel function that can be calculated in a closed form on the original feature space. The kernel encapsulates incremental changes between subspaces, and these changes are the basis for the differences and commonalities between the two domains. Therefore, the learning algorithm uses this kernel to derive a low-dimensional representation of domain invariance. The main idea is shown in fig .I-D3.

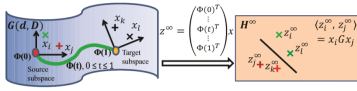


Fig. 3.

4) *Transfer Component Analysis (TCA)*:

5) *Easy Transfer Learning (EasyTL)*:

E. Deep Transfer Learning Methods

1) *Deep Adaptation Network (DAN)*: »»»» Stashed changes

II. EXPERIMENTS

In this part, we will show the experimental results and comparative analysis of the results through two types of traditional transfer learning methods and deep transfer learning methods.

A. Baseline

Before using transfer learning methods, we applied linear SVM and rbf kernel SVM directly and used the results as baseline of this experiment. Besides, we used *GridSearchCV* to find the optimal value of parameters. The results are shown in Table .I. And we visualize the source domain and target domain, the result is shown in the fig. 4.

TABLE I
THE RESULT OF BASELINE

dataset \ result	accuracy	C	kernel
Art->RealWorld	0.7484	10.0	rbf
Clipart->RealWorld	0.6577	0.01	linear
Product->RealWorld	0.7294	10.0	rbf

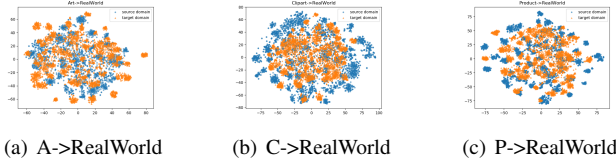


Fig. 4. baseline

B. Traditional Transfer Learning Methods

1) *KMM*: In this experiment, we used the KMM method to assign different weights on source domain samples in order to make the probability distribution of the weighted source and target domains as close as possible. And our experiment results are shown in Table II.

From the results, we can see that rbf and linear KMM perform similarly, and there is almost no improvement compared to baseline. So we visualized the result of KMM for Art-Realworld in fig .II-B1. We speculate that the reason why the experimental performance has hardly improved is that the

weights given by KMM to most samples are similar, which may not help to narrow the sample distribution of the source domain and target domain. In addition, the sample distribution of the source domain and target domain is not particularly different, and may be one of the reasons.

TABLE II
THE RESULT OF KMM

dataset \ result	accuracy	kernel
Art->RealWorld	0.7528	linear
Clipart->RealWorld	0.6518	linear
Product->RealWorld	0.7296	linear
Art->RealWorld	0.7528	rbf
Clipart->RealWorld	0.6513	rbf
Product->RealWorld	0.7294	rbf

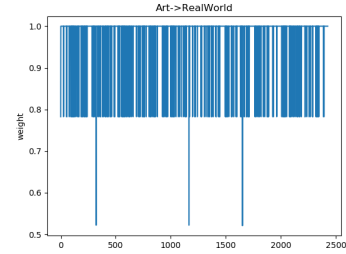


Fig. 5. Samplpe weights of Art-Realword of RBF

2) *CORAL*: In this experiment, we used the CORAL method to minimize the second-order distance between source domain and target domain. And our experiment results are shown in Table III.

From the results we can see that only the experiment results of Product-Realworld are slightly better than the baseline. We visualize the source domain processed by the CORAL method and compare it with the baseline. We can't find that the obvious data distribution is getting closer. We speculate that the reason CORAL is not performing well is that it is not suitable for no-deep models.

TABLE III
THE RESULT OF CORAL

dataset \ result	accuracy
Art->RealWorld	0.7381
Clipart->RealWorld	0.6513
Product->RealWorld	0.7369

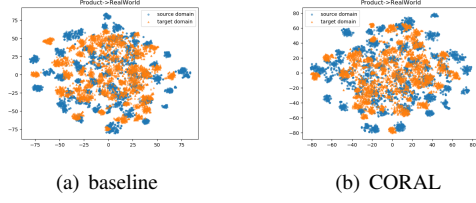


Fig. 6. baseline and CORAL for Product-Realworld

3) *GFK*: In this experiment we changed the dimension of geodesic flow kernel for comparative experiment. The experimental results are shown in the Table IV.

From the results we can see that the dimension of geodesic flow kernel will affect the experiment, and the optimal dimension in this project is 128, that is, the source domain and target domain can maintain maximum consistency in the 128-dimensional subspace. For the three data sets, GFK's experimental results have improved compared to the baseline. We visualize the source domain and target domain after GFK processing, and compare with the baseline, as shown in the Fig .7. We can find that GFK makes the sample distribution of source domain and target domain indeed closer.

TABLE IV
THE RESULT OF GFK

dataset \ result	accuracy	dimension
Art->RealWorld	0.7190	32
Clipart->RealWorld	0.6336	
Product->RealWorld	0.7117	
Art->RealWorld	0.7456	64
Clipart->RealWorld	0.6561	
Product->RealWorld	0.7335	
Art->RealWorld	0.7537	128
Clipart->RealWorld	0.6598	
Product->RealWorld	0.7310	
Art->RealWorld	0.7482	256
Clipart->RealWorld	0.6566	
Product->RealWorld	0.7300	
Art->RealWorld	0.7475	512
Clipart->RealWorld	0.6575	
Product->RealWorld	0.7284	
Art->RealWorld	0.7475	1024
Clipart->RealWorld	0.6580	
Product->RealWorld	0.7296	

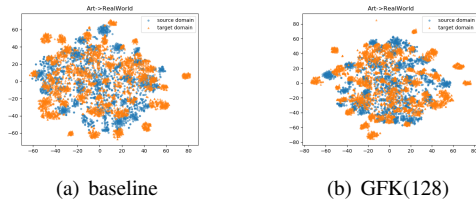


Fig. 7. baseline and GFK for Art-Realworld

C. Transfer Component Analysis (TCA)

D. Easy Transfer Learning (EasyTL)

E. Deep Adaptation Network (DAN)

III. CONCLUSION

[6]

REFERENCES

- [1] S. J. Pan, I. W. Tsang, J. T. Kwok, and Q. Yang, "Domain adaptation via transfer component analysis," *IEEE Transactions on Neural Networks*, vol. 22, no. 2, pp. 199–210, 2011.
- [2] J. Wang, Y. Chen, H. Yu, M. Huang, and Q. Yang, "Easy transfer learning by exploiting intra-domain structures," 2019.
- [3] M. Long, Y. Cao, J. Wang, and M. I. Jordan, "Learning transferable features with deep adaptation networks," 2015.
- [4] A. Gretton, A. Smola, J. Huang, M. Schmittfull, K. Borgwardt, and B. Schölkopf, "Covariate shift by kernel mean matching," *Dataset shift in machine learning*, vol. 3, no. 4, p. 5, 2009.
- [5] B. Gong, Y. Shi, F. Sha, and K. Grauman, "Geodesic flow kernel for unsupervised domain adaptation," in *2012 IEEE Conference on Computer Vision and Pattern Recognition*. IEEE, 2012, pp. 2066–2073.
- [6] D. G. Lowe, "Object recognition from local scale-invariant features," in *Proceedings of the seventh IEEE international conference on computer vision*, vol. 2. Ieee, 1999, pp. 1150–1157.